Composites Science and Technology 153 (2017) 168–177

Contents lists available at ScienceDirect

Composites Science and Technology

journal homepage: http://www.elsevier.com/locate/compscitech

Anti-impact response of Kevlar sandwich structure with silly putty core

Chenhui Xu [a], Yu Wang [a], Jie Wu [a], Shichao Song [a], Saisai Cao [a], Shouhu Xuan [a, *], Wanquan Jiang [b], Xinglong Gong [a, **]

[a] CAS Key Laboratory of Mechanical Behavior and Design of Materials, Department of Modern Mechanics, University of Science and Technology of China (USTC), Hefei 230027, PR China
[b] Department of Chemistry, USTC, Hefei 230026, PR China

ARTICLE INFO

Article history:
Received 28 June 2017
Received in revised form
5 September 2017
Accepted 20 October 2017

Keywords:
Flexible composites
Sandwich
Aramid fiber
Polymer-matrix composites (PMCs)
Impact behavior

ABSTRACT

A soft sandwich structure consisting of two layer Kevlar face sheets and a silly putty (SP) core was fabricated. The storage modulus of SP, which was prepared by dispersing $CaCO_3$ particles into polyborodimethylsiloxane, increased by two to three orders of magnitude with increasing of the shear frequency. The higher $CaCO_3$ content resulted in better shear-hardening behavior, which further enhanced the anti-impact performance of the sandwich structure. When the impact velocity was below 110 m/s, all energy was dissipated by the sandwich structure and the maximum energy dissipation was 20.8 J, represented a 60% increment than the neat Kevlar. Importantly, under the same impact energy, the energy dissipation of the sandwich structure under ballistic impact was 63% higher than under low velocity impact, which must be due to the shear-hardening nature. The mechanism of the excellent protection performance was discussed. The sensitivity to loading rate and reliable energy dissipation of the soft sandwich structure widely broad its practical applications.

1. Introduction

Over the past several decades, because of the increasingly frequent global terrorism and civil conflicts, body armors which can protect a person from the damage caused by weapons or projectiles have become a research hotspot. Traditional personal body armors are made of metals [1], ceramics [2] and transparent glasses [3], thus they are heavy, rigid and bulk. Limited by the shortage of their flexibility and mobility, these traditional body armors can hardly protect arms or legs. Therefore, more and more attentions are focused on reducing the weight and improving the flexibility of personal body armor while ensuring the same protective effect [4–6].

Kevlar, a kind of aromatic polyamide fiber, has been widely used in soft body armors as a base material because of its high strength, toughness, and modulus, light weight and stability [7,8]. In order to get better performance, many researches were conducted on tailoring the structure and composition of Kevlar. To achieve the high protection performance, Hwang et al. [5] increased the friction between yarns of the aramid fabric through the growth of zinc oxide nanowires on the fiber surface so as to enhance the ballistic resistance. Haro et al. [9] synthesized hybrid composite laminates for armor protection, which consist of layers of aluminum alloy and Kevlar fibers impregnated with shear thickening fluid and epoxy resin. Due to the smart structure and composition, the final products presented better protection than the neat Kevlar precursor.

Among various structures of the Kevlar based body armor, the shear thickening fluids (STFs) impregnated Kevlar fiber is the most attracting one. STFs are a kind of smart materials whose apparent viscosity can be dramatically increased when subjected to a high-speed impact loading. They can recover immediately after removing the impact. Due to their reversible and particularly sensitive rate-dependent shear thickening characteristic, the STFs possess high potential in energy dissipation and personal body protection [10–12]. Lee et al. [13] found the ballistic resistance of Kevlar fabric could be enhanced after impregnating with SiO_2-based STFs. To investigate the enhancing mechanism, Lee et al. [14] investigated the effect of the particle size in STFs and Kalman et al. [15] studied the influence of particle hardness in STFs impregnated

* Corresponding author.
** Corresponding author.
E-mail addresses: xuansh@ustc.edu.cn (S. Xuan), gongxl@ustc.edu.cn (X. Gong).

https://doi.org/10.1016/j.compscitech.2017.10.019
0266-3538/

fabrics. The numerical simulation was also conducted by Park et al. [16] to study the friction effects in STFs impregnated Kevlar fabric under the high velocity impact.

Recently, because of the instability of fluidic STFs, some researches have been focused on a new shear-hardening polymer - silly putty (SP), which is a viscoelastic material sensitive to strain rate [17–20]. It behaves like a soft plasticine in nature state but becomes very hard when suffering an external impact. Recently, Liang et al. [21] applied SP in a shock transmission unit which provided a free motion under slowly applied loads and a rigid link under impact loads. Jiang et al. [22] tested the SP composite by falling weight impact and split Hopkinson pressure bar experiments. It was found that SP could store up to 23% of the impact energy and showed solid characters at high strain rate. To broad the application of SP in protection, Wang et al. [23] incorporated SP into polyurethane sponge. The results indicated that the impact force could be reduced by 2 orders even under 26 cycles of continuous dynamic impact loading. In consideration of their high performance, the composite structures composed of Kevlar and SP will be favorable for body armor. Unfortunately, few work based on the Kevlar/SP has been reported.

Sandwich structure is a kind of composite component, which features a light weight core placed between two high strength thin plates or skins. It is extensively used to dissipate energy and protect a system from ballistic threats. The plates, which are still rigid and unsuited to personal wearing, typically include aluminum or other rigid fiber reinforced polymer. The core of the sandwich structure is usually made of the material with low density, high stiffness and energy absorption, such as metallic foam [24], fiber [25], polymer [26] and other light materials [27], which can enhance the strength and energy dissipation of the sandwich structure. Considering the high flexibility, easy sealing and rate-sensitivity characteristics of SP and the high strength, light weight and soft of Kevlar, the sandwich structure combining of Kevlar fabrics with SP core can not only become a comfortable light material but also provide reliable protective and energy dissipation performance as a personal body armor.

In this work, the anti-impact performance of a soft sandwich structure consisting of two layer Kevlar face sheets and a SP core was studied through ballistic and low velocity impact tests. The effect of $CaCO_3$ contents on the mechanical properties of the SP and Kevlar/SP were investigated. The storage modulus of SP under various shear frequency was measured for indicating the sensitivity to strain rate. Ballistic impact tests of the Kevlar/SP were conducted at the velocity ranging from around 90 to 150 m/s. The process of deformation and destruction was recorded by the high-speed video camera at 50,000 fps. Additionally, the low velocity impact test was conducted at the same impact energy as the ballistic impact. The difference of the two impact test results was carefully discussed. At last, the possible mechanism was proposed to analyze the rate dependent protective property of the Kevlar/SP. This sandwich structure with Kevlar face sheets and SP core declared excellent energy dissipation to ballistic threats and this soft wear possessed the huge potential in personal body armors.

2. Materials and methods

2.1. Materials and preparation

Boric acid, dimethyl silicone oil, ethanol, benzoyl peroxide(BPO) (Sinopharm Chemical Reagent Co. Ltd, Shanghai, China) were raw materials to synthesize SP matrix – polyborodimethylsiloxane (PBDMS). The 1250 mesh $CaCO_3$ (Lingdong Chemical Co. Ltd, Shanghai, China) was used as reinforced particles. HTV silicone rubber (type MVQ 110-2 from Dong Jue Fine Chemicals Co. Ltd, Nanjing, China) was the control group in contrast with SP. Kevlar fabric (Junantai Protection Technologies Co. Ltd, Beijing, China) was a type of plain-woven high-performance aramid.

Firstly, the boric acid was heated at 160 °C for 2 h to gain pyroboric acid. Then, pyroboric acid and dimethyl silicone oil (mass ratio 2:15) and 15 ml of ethanol were mixed in a beaker and heated for about 7 h at high temperature. Subsequently, the BPO (as the cross-linking agent) and different contents of $CaCO_3$ particles were added to the above product by the internal mixer (HL-200, Jilin University Scientic and Teaching Instrument Factory, Jilin, China). At last, the mixture was sulfurized for 2 h at 110 °C to obtain SP. The mass fractions of $CaCO_3$ were kept at 0, 20, 35, and 50 wt%, respectively. For simplicity, the SP with $CaCO_3$ particles are defined as SP-$CaCO_3$-X%, where X is the mass fraction of the $CaCO_3$ particles.

Fig. 1(a) and (b) show the schematic of the fabrication procedure and the composition of the sandwich structure. The front and rear face sheets were both single layer Kevlar fabric with an areal density of 200 $g \cdot m^{-2}$ and the edges were stitched by sewing threads to maintain the soft core inside the structure. Five different components of sandwich core (kept at 30 g) were used in this work: HTV silicone rubber (as the control group) and SP with four different contents of $CaCO_3$ particles (as mentioned above). The impacted part was a square with a side length of 127 mm. More parameters of the sandwich structure are shown in Table 1.

2.2. Characterization

Rheological properties of SP and HTV silicone rubber were studied using a torque rheometer (Physica MCR 301, Anton Paar Co., Austria). The dimension of the tested samples was Φ20 mm × 1 mm. A frequency sweep test was carried out with a parallel plate (Φ20 mm). The frequency was varied from 0.1 Hz to 100 Hz at 25 °C with a strain of 0.1%. The Kevlar fabrics in the sandwich structure were investigated by the SEM (FEI, type: XL-30 ESEM).

2.3. Ballistic impact testing

The experimental configuration consisted of five components: a gas gun as the launcher, a laser velocimeter to measure the impact velocity of the projectile, a steel frame for the target sample, a projectile catcher, and a high-speed video camera (Fig. 2(a)). According to the NIJ Standard 0101.04 [28] and MIL-DTL-46593B [29], a 44 grain (2.85 g) chisel-nosed steel fragment simulating projectiles (FSP) was used (Fig. 2(b)) and its impact velocity varied from 90 m/s to 150 m/s. A heavy steel frame was fixed on the basement to prevent violent vibration and the target sample was four edges clamped tightly (Fig. 2(c and d)). The high-speed video camera (FASTCAM SA5 1000 k-M3, Photron) was used to capture the deformation and destruction process of the rear face and record the projectile position for calculating the residual velocity. The target sample was placed in close with the muzzle (15 cm) so that the yaw and velocity decay of the FSP could be neglected.

2.4. Low velocity impact testing

Low velocity impact experiment (Fig. 3) was conducted by a drop tower test device (ZCJ1302-A, MTS Co. Ltd, China). A 1.97 kg impactor had the same shape and dimension with FSP expect length. During the impact, the accelerometer collected the accelerometer signals of drop tower and transformed them into electric signals. Finally, through the charge amplifier, the signals were recorded by the oscilloscope.

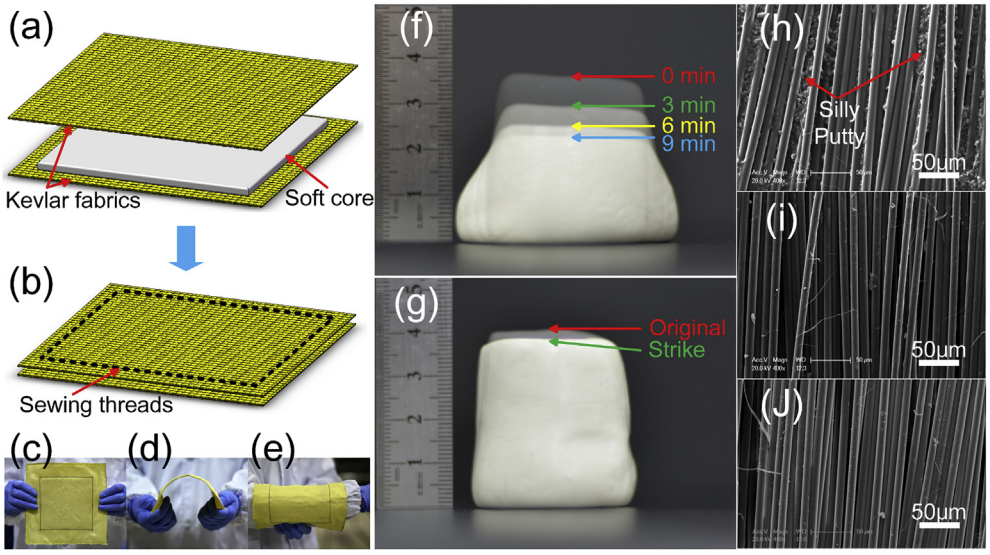

Fig. 1. Schematic of the fabrication procedure and morphologies of the sandwich structure: (a, b) preparation process; (c) flat; (d) bend; and (e) cover on the arm. Impact stiffening behavior (SP-$CaCO_3$-20%): (f) deformation under self-weight; (g) deformation resistance under impact. SEM images: (h) the interface between Kevlar and SP; (i) the outer surface; (j) the neat Kevlar.

Table 1
The parameters of the sandwich structure.

Sample no	Component	Mass (g)	Areal Density ($kg \cdot m^{-2}$)	Thickness (mm)
K	Kevlar/Kevlar	6.46	0.40	0.50
SR	Kevlar/HTV Silicon Rubber/Kevlar	36.46	2.26	2.44
S0	Kevlar/SP-$CaCO_3$-0%/Kevlar	36.46	2.26	2.30
S20	Kevlar/SP-$CaCO_3$-20%/Kevlar	36.46	2.26	2.04
S35	Kevlar/SP-$CaCO_3$-35%/Kevlar	36.46	2.26	1.88
S50	Kevlar/SP-$CaCO_3$-50%/Kevlar	36.46	2.26	1.75

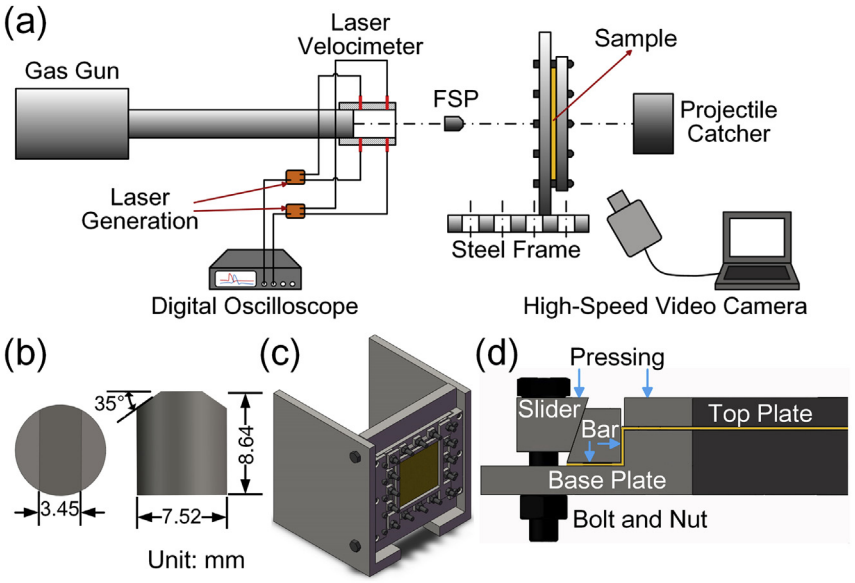

Fig. 2. Schematic of the Ballistic impact testing system: (a) the experimental configuration; (b) dimensions of the FSP; (c) three-dimensional view of the steel frame; (d) section view showing how the sample is tightly clamped.

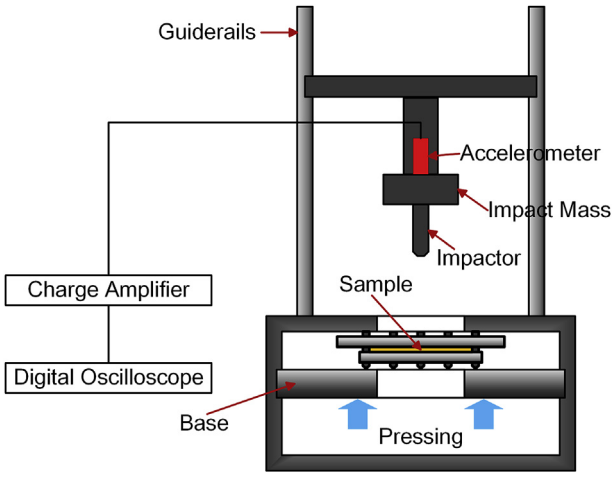

Fig. 3. Schematic of the drop tower test device for low velocity impact experiment.

3. Results and discussion

3.1. Characterization of SP and the sandwich structure

The mechanical properties of SP and HTV silicone rubber were characterized at first. The results showed the storage modulus (G') of all samples increased with increasing shear frequency (Fig. 4). For example, the G' of SP-$CaCO_3$-0% was measured to be 1.32×10^{-4} MPa at the initial frequency of 0.1 Hz. When the shear frequency increased, the G' increased rapidly and finally reached a steady value about 0.71 MPa at the maximum frequency of 100 Hz. The G' increased by about 4 orders of magnitude. However, the G' of HTV silicon rubber changed from 2.69×10^{-3} MPa to 0.12 MPa and only increased by about 2 orders of magnitude. This difference illustrates that SP owns a higher shear-hardening behavior. Similar to the previous report [17,18,20–23], SP looks like a plasticine and possesses the typical cold-fluidic characteristic (Fig. 1(f and g)). Under a sudden impact, SP transforms from the viscoelastic state to the elastic state, indicating the unique shear-hardening effect.

To compare the shear-hardening effects under oscillation shearing loading, a relative shear-hardening effect (RSHe) is defined in Eq. (1) [30]:

$$\mathrm{RSHe} = \frac{G'_{max} - G'_{min}}{G'_{min}} \times 100\% \quad (1)$$

where G'_{max} and G'_{min} is the storage modulus of the sample induced by the maximum frequency and the initial frequency, respectively. More details are listed in Table 2. When the contents of $CaCO_3$ particles in SP are increased, the initial and maximum storage modulus both increase. Correspondingly, the shear-hardening effect of the final SP decreases due to the quick increase of the initial storage modulus. Importantly, it is found that SP is more sensitive to strain rate than HTV silicone rubber.

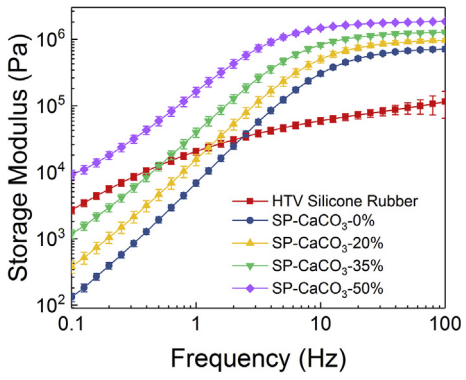

Fig. 4. The curves of storage modulus versus shear frequency of different materials.

Fig. 1 (h) and (i) show the SEM images of the interface between Kevlar fabric and SP and the fabric outer surface. Before the SEM observation, the fabric was separated from the sandwich structure. Obviously, SP adheres to fabrics on the interface and immerses in the gaps. But the outer face of Kevlar is just same to the surface of the neat Kevlar (Fig. 1 (j)). It declares that the soft core can be well kept within the sandwich structure and will not seep out.

3.2. Ballistic impact testing

3.2.1. Residual velocity and energy dissipation

In the ballistic impact testing, the projectile was launched by a gas gun to penetrate the sandwich structure. A laser velocimeter and a high-speed video camera were used to measure the incident velocity (V_i) and the residual velocity (V_r). Then, the V_r-V_i curves were obtained (Fig. 5(a)). The V_r increases with the V_i increasing but the increasing rate is reduced. Clearly, the performance of ballistic resistance of each samples is different. The ballistic limit velocity (V_{bl}), the minimum incident velocity as the projectile penetrating samples, was used to quantify the distinction. The V_{bl} for Kevlar/SP/Kevlar samples (S50, S35, S20, S0) were measured to be 116.4, 115.5, 113.0, and 110.1 m/s. These value are much higher than the V_{bl} of Kevlar/HTV/Kevlar (89.5 m/s). Interestingly, the V_{bl} increases with increasing of the contents of $CaCO_3$ particles in SP. This is similar to the result of G'_{max} (Fig. 4 and Table 2). The sample with higher G'_{max} owns larger V_{bl}, which also exhibits stronger resistance to the ballistic impact. The ballistic resistance of Kevlar/Kevlar was tested, and the V_{bl} (92.6 m/s) is slightly larger than the V_{bl} of Kevlar/HTV/Kevlar but far less than the V_{bl} of Kevlar/SP/Kevlar. It demonstrates that the SP core can effectively strengthen the ballistic resistance capability, but the performance will be weakened when the core is HTV silicone rubber.

In this study, the performance of ballistic resistance was also quantified by calculating the energy dissipation and energy dissipation ratio, based on the incident velocity and residual velocity of the projectile. The projectile is assuming to be non-deformable and related parameters are described as follows [9]:

$$E_{dis} = E_i - E_r \quad (2)$$

$$\eta = \frac{E_{dis}}{E_i} \times 100\% \quad (3)$$

$$E_i = \frac{1}{2}mV_i^2,\ E_r = \frac{1}{2}mV_r^2 \quad (4)$$

here, V_i and V_r are the incident velocity and residual velocity, E_i and E_r are the kinetic energy of the projectile before and after

Table 2
The G'_{max}, G'_{min} and RSHe% of samples in the frequency tests.

Sample	G'_{min} (MPa)	G'_{max} (MPa)	RSHe (%)
HTV Silicon Rubber	2.69×10^{-3}	0.12	4189%
SP-$CaCO_3$-0%	1.32×10^{-4}	0.71	540,364%
SP-$CaCO_3$-20%	3.82×10^{-4}	0.97	253,192%
SP-$CaCO_3$-35%	1.19×10^{-3}	1.28	107,525%
SP-$CaCO_3$-50%	9.26×10^{-3}	1.86	19,984%

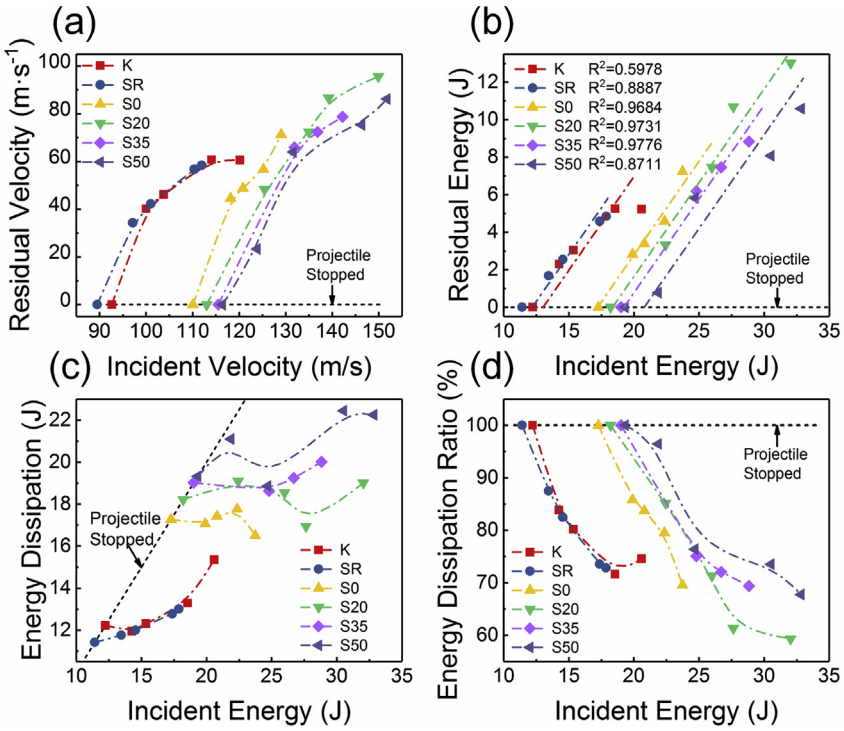

Fig. 5. Ballistic impact testing results of different samples: (a) the residual velocity of the projectile at different incident velocities; (b) the residual kinetic energy of the projectile, (c) the energy dissipation, and (d) the energy dissipation ratio of the samples to incident kinetic energy.

penetrating, and E_{dis} and η are the energy dissipation and energy dissipation ratio, respectively.

Fig. 5(b) presents the relationship between incident energy (E_i) and residual energy (E_r). For each sample, the coefficients of determination (R^2) are shown in Fig. 5(b) and the linear fitting results with a fixed slope of 1 illustrate the positive correlation of E_r with the E_i as described in Eq. (2). Such relationship declares the E_{dis} is approximately a constant in the ballistic impact which is similar to that the G' finally plateaus at high shear frequency. Based on Eq. (2), the energy dissipations of Kevlar/SP/Kevlar (S50, S35, S20, S0) were calculated to be 20.8, 19.2, 18.4, and 17.2 J. Kevlar/SP/Kevlar can dissipate much more kinetic energy than Kevlar/HTV/Kevlar (12.2 J) and Kevlar/Kevlar (13.0 J). More importantly, it is found that the more $CaCO_3$ particles in SP, the more energy is dissipated.

Also, the curves of the energy dissipation and the energy dissipation ratio to initial kinetic energy are displayed in Fig. 5(c) and (d). In this work, the low resolution and high frame rate of the high-speed photographs and the friction between the projectile and the launcher caused the unavoidable errors in the velocity measurement. As a result, with increasing of the E_i, the E_{dis} of each sample fluctuates around the calculated E_{dis} (Fig. 5(c)), and the η of each sample decreases (Fig. 5(d)). Even so, the differences of E_{dis} and η of different samples illustrate that Kevlar/SP/Kevlar can provide better protection performance than others and the effect of protection is enhanced with the more $CaCO_3$ particles in SP. After comparing the V_r at the same V_i of 120 m/s, the E_r, E_{dis}, and η to the same E_i of 20.52 J (Fig. S1 (a) and (b)), a same conclusion was obtained.

3.2.2. Deformation and destruction

The high-speed video camera can capture the flight path and velocity of the projectile and record the deformation and destruction process of the sandwich structure (Fig. 6). The longitudinal stress wave propagates along the thickness direction and the transverse stress wave spreads to the surroundings in the plane [31]. At the beginning of the ballistic impact, the geometry of the deformation caused by the impact was like a small pyramid because the transverse stress wave was too late to propagate to the boundary. Then, the pyramid became bigger with the stress wave propagating during the movement of the projectile. Finally, the Kevlar fabrics and the core materials were destructed or thoroughly penetrated which dissipated the incident energy.

Fig. 6(a–b) and Movie S1-S2 show two samples with different cores at the near impact velocity. The Kevlar/HTV/Kevlar was penetrated thoroughly and the projectile continued to move at the velocity of 58.3 m/s (Fig. 6(a), Movie S1). The projectile could not penetrate Kevlar/SP-$CaCO_3$-20%/Kevlar and only cause a small area destruction (Fig. 6(b), Movie S2). In comparison to Kevlar/HTV/Kevlar, the ballistic resistance performance of Kevlar/SP-$CaCO_3$-20%/Kevlar is much stronger at the same incident velocity. Here, the thickness of Kevlar/SP-$CaCO_3$-20%/Kevlar is thinner than Kevlar/HTV/Kevlar, although their area density and mass are same (Table 2).

Supplementary data related to this article can be found at https://doi.org/10.1016/j.compscitech.2017.10.019.

Fig. 6(c) and Movie S3 shows the anti-impact process of Kevlar/SP-$CaCO_3$-20%/Kevlar at the velocity of 125 m/s. Here, though it was penetrated by the projectile, the high velocity also means it can resist the impact more effectively than Kevlar/HTV/Kevlar. The destruction processes for the two samples are obviously different. In Fig. 6(a) and Movie S1, the impact of the projectile caused a small hole in the Kevlar fabric, and only a small amount of silicone rubber was taken away. However, a lot of SP was crumbled and ejected like powders (Fig. 6(c), Movie S3). It clearly demonstrates the energy was dissipated through the SP core damage: under the ballistic impact, SP transformed from soft state to solid state, the transverse stress led to the destruction of SP around the hole and then the

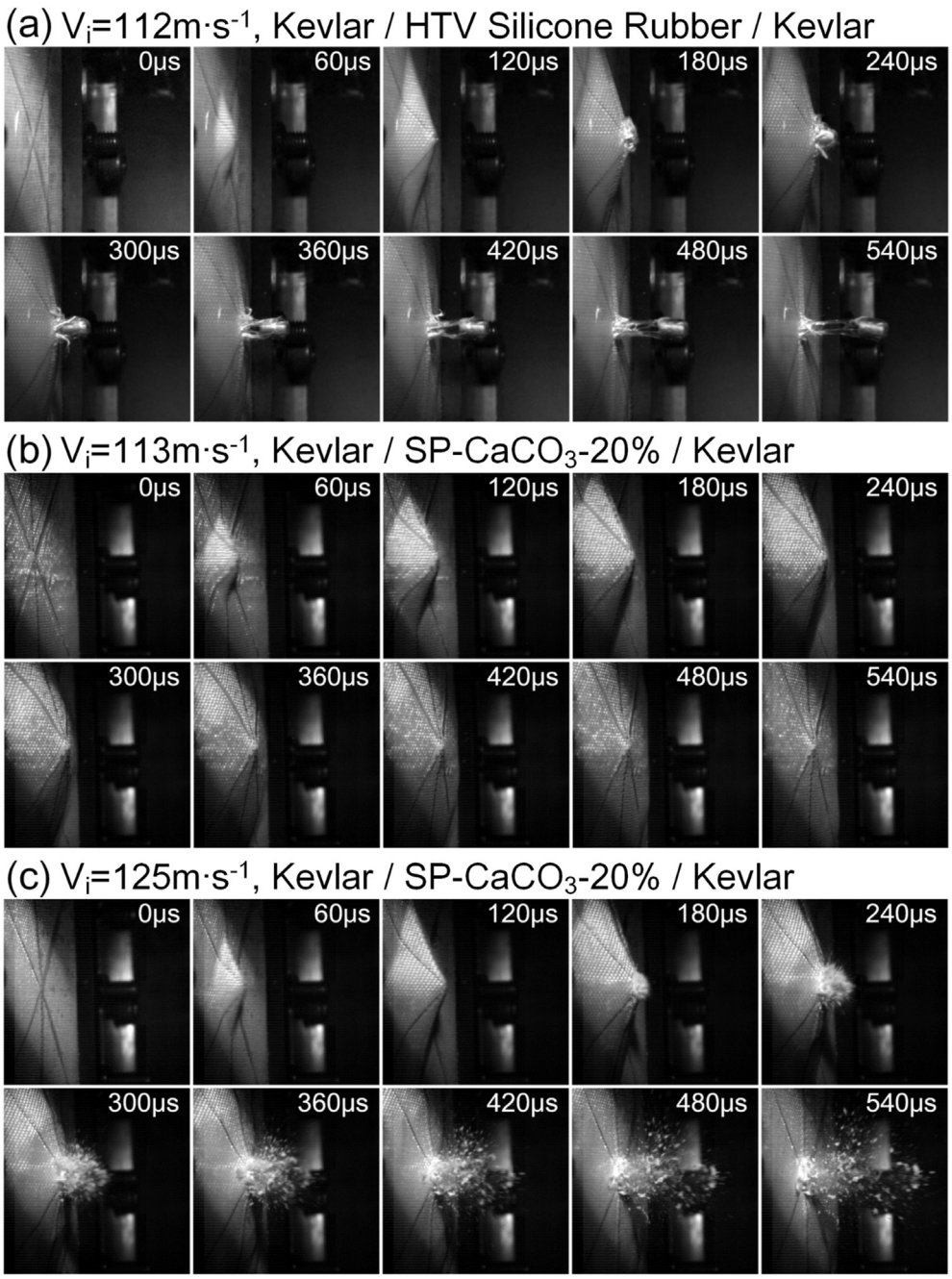

Fig. 6. The high-speed photographs of the deformation and destruction of the samples in the ballistic impact process: (a) Kevlar/HTV Silicone Rubber/Kevlar at the incident velocity of 112 m/s, (b) Kevlar/SP-$CaCO_3$-20%/Kevlar at the impact velocity of 113 m/s, and (c) 125 m/s.

ejecta moved fast with absorbed energy. These mechanisms lead to the huge energy dissipation contribution of the SP core.

Supplementary data related to this article can be found at https://doi.org/10.1016/j.compscitech.2017.10.019.

3.3. Low velocity impact testing

3.3.1. Acceleration and velocity history

In the low velocity impact testing, a drop tower was used to impact the samples. The acceleration signal was measured by the accelerometer and the initial velocity was calculated by the formula of the free falling body (Eq. (5)). The velocity during the impact process was calculated from the integration of acceleration signals (Eq. (6)).

$$V_0 = \sqrt{2gh} \tag{5}$$

$$V_t = V_0 + \int_0^t a dt \tag{6}$$

Here, g is the acceleration of gravity being 10 m s^{-2}, h is the height of the drop tower from the initial position to the contact position, a is the acceleration, V_0 is the initial impact velocity and V_t is the velocity during the impact velocity.

The acceleration and velocity history of the drop tower for

Kevlar/SP-$CaCO_3$-20%/Kevlar were given as an example (Fig. 7(a)). The tower dropped from 924 mm. After contacting the sample, the acceleration increased slowly and then the increasing rate became faster, representing the deformation of the sample became larger. When the acceleration reached to the maximum, the curve appeared to fluctuate because some of the yarns were broken. With the number of broken yarns increasing, the acceleration dropped to zero rapidly and then the impactor penetrated the sample. Subsequent fluctuations were caused by the vibration of the impact mass. Consequently, the velocity of the tower was firstly reduced slowly and then dropped rapidly to the minimum value. Fig. 7(b) shows the acceleration signals of the tower impacting different samples dropping from the height of around 1000 mm. In the first 2 ms, the acceleration curves are coincident because the same Kevlar layer played a major role in the resistance. After this, the core materials began to show different resistance effects, which led to different accelerations and penetrate time. The maximum accelerations of Kevlar/SP/Kevlar (S50, S35, S20, S0), Kevlar/HTV/Kevlar and Kevlar/Kevlar are 1780, 1488, 1431, 1365, 938 and 1352 m s^{-2}, respectively (Fig. 7(c)). It declares that the resistance of SP with higher content of $CaCO_3$ particles is stronger. And the impact time of Kevlar/SP/Kevlar is longer than Kevlar/HTV/Kevlar and Kevlar/Kevlar, so they can dissipate more energy.

3.3.2. Comparison of energy dissipation

In low velocity impact testing, the incident energy (E_i) and the energy dissipation (E_{dis}) were calculated by Eqs. (2) and (4). The incident velocity was defined as the initial velocity described in Eq. (5) and the residual velocity was the minimum velocity during the impact process (Fig. S2). The E_{dis} under low velocity and ballistic impact as a function of E_i is shown in Fig. 8. The E_{dis} of each sample is approximately a constant both in low velocity and ballistic impact testing as mentioned above. In the case of low velocity impact, there is only a slight improvement about the E_{dis} of Kevlar/SP/Kevlar compared to Kevlar/Kevlar, because SP still behaves in a soft state. However, due to the unique shear-hardening effect, SP turns into solid-like state under ballistic impact, so the E_{dis} under ballistic impact is much higher.

Furthermore, the average energy dissipation ($\overline{E_{dis}}$) of different samples was calculated (Fig. 9(a)). The relationship between the E_{dis} and different samples under low velocity impact is similar to the situation under ballistic impact. For Kevlar/SP/Kevlar, the $\overline{E_{dis}}$ increases with the increasing of $CaCO_3$ content in SP, indicating an enhancing effect. Fig. 9(b) demonstrates that the difference between ballistic and low velocity impact (ΔE_{dis}) reflects the sensitivity of the sandwich to the strain rate and the component of the core. When the samples are impacted by the high-speed projectile, the performance on energy dissipation is more outstanding so the values of ΔE_{dis} are all positive. The ΔE_{dis} of Kevlar/Kevlar is the lowest, which declares that the ΔE_{dis} is mainly contributed by the core materials due to the shear-hardening effect. In order to identify the energy dissipation contribution of sandwich components, the energy dissipation contribution of the Kevlar face sheets is assuming to be equal to the energy dissipation of Kevlar/Kevlar. Thus, the energy dissipation contribution of the sandwich materials is calculated by Eq. (7):

$$E_{dis(core)} = E_{dis} - E_{dis(K)} \tag{7}$$

Here, $E_{dis(core)}$ is the energy dissipation contribution of the sandwich core, E_{dis} is the energy dissipation of the sandwich, and the $E_{dis(K)}$ is the energy dissipation of Kevlar/Kevlar.

The SP with different $CaCO_3$ content can contribute to extra energy dissipation (Fig. 9(c)). In the case of low velocity impact, SP contributed about 2 J energy dissipation in the soft state. But under ballistic impact, SP turned into solid-like state rapidly and caused vast extra energy dissipation. Especially the SP-$CaCO_3$-50%, it

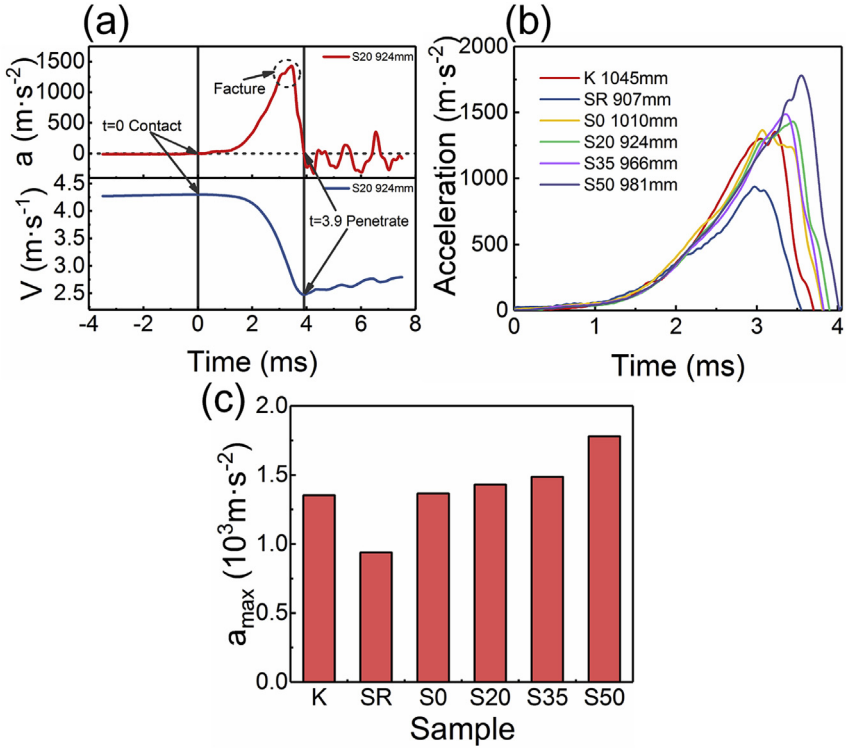

Fig. 7. The acceleration and velocity history of the drop tower: (a) impacting Kevlar/SP-$CaCO_3$-20%/Kevlar sample from 924 mm; (b) the acceleration signals of the tower dropping from around 1000 mm to different samples and (c) the maximum acceleration.

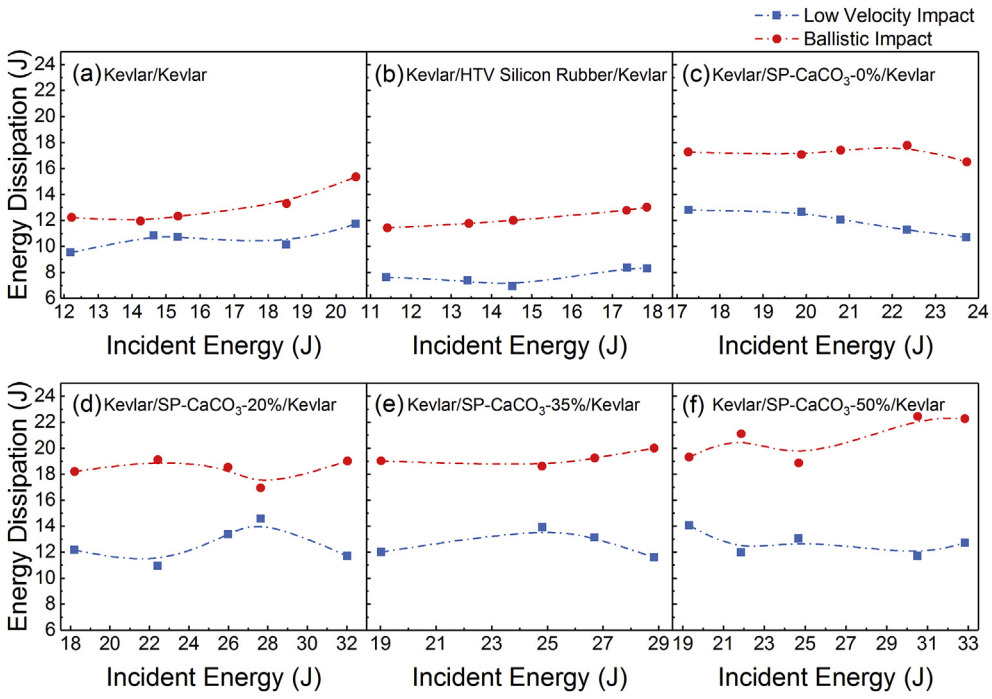

Fig. 8. Comparison of the energy dissipation under the ballistic and low velocity impacts: (a) Kevlar/Kevlar; (b) Kevlar/HTV Silicone Rubber/Kevlar; (c) Kevlar/SP-$CaCO_3$-0%/Kevlar; (d) Kevlar/SP-$CaCO_3$-20%/Kevlar; (e) Kevlar/SP-$CaCO_3$-35%/Kevlar; (f) Kevlar/SP-$CaCO_3$-50%/Kevlar.

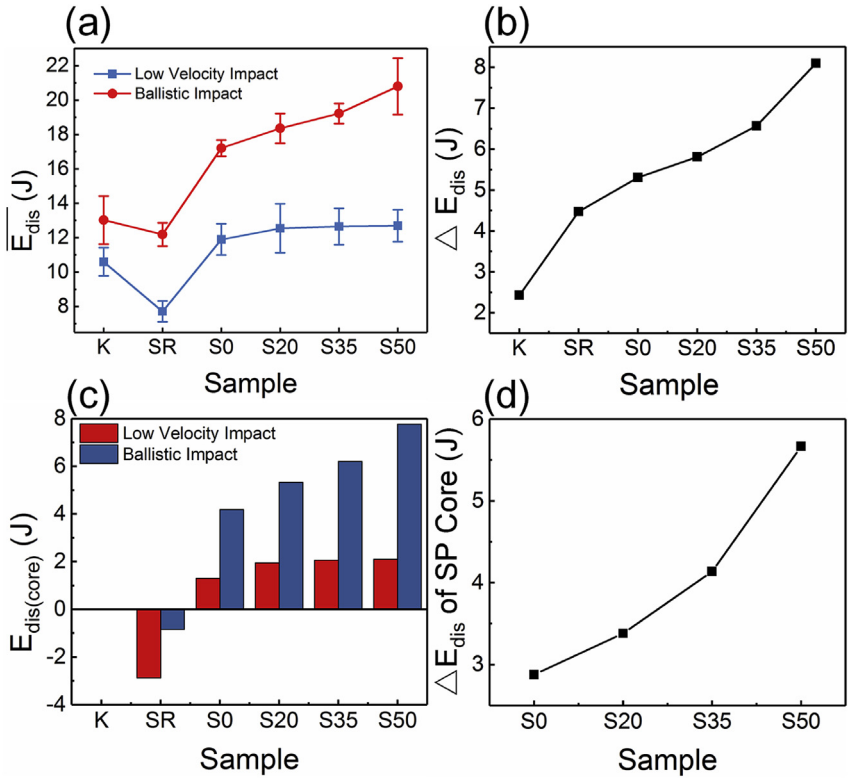

Fig. 9. (a) Comparison of the average energy dissipation ($\overline{E_{dis}}$) and (b) the difference of the average energy dissipation (ΔE_{dis}) between the ballistic and low velocity impact; (c) the energy dissipation contribution of different sandwich soft cores ($E_{dis(core)}$); (d) the difference of the energy dissipation (ΔE_{dis}) contribution of SP cores between the ballistic and low velocity impact.

contributed additional 60% (7.8 J) energy dissipation compared to Kevlar/Kevlar. Therefore, it can be concluded that the energy absorbed is dissipated through skin and core damage. Under ballistic impact, the SP core contributed more influence on the energy

dissipation than in the low velocity impact (Fig. 9(d)). Remarkably, the contribution of HTV silicone rubber in Kevlar/HTV/Kevlar was negative. The HTV silicone rubber weakened the capacity of impact resistance. This result demonstrates the unique protective ability and energy dissipation contribution of SP exactly.

The ΔE_{dis} of sandwiches increases remarkably with increasing the content of $CaCO_3$ particles (Fig. 9(b)), which is similar to the function of the G'_{max} and the weight of $CaCO_3$ (Fig. 4 and Table 2). Fig. 9(d) presents the difference of the energy dissipation contribution of SP cores between ballistic impact and low velocity impact (ΔE_{dis} of SP cores). Clearly, with increasing of the $CaCO_3$ content, the ΔE_{dis} of SP cores increases, demonstrating that more impact energy can be dissipated by the SP with higher shear-hardening effect. Due to unique shear-hardening effect, the SP core can significantly improve the strength of sandwich structure when suffering ballistic impact. With increasing of the filled $CaCO_3$ particles in the SP, the dissipation effect increased, which must be originated from the increasing friction between the projectile and $CaCO_3$ particles, especially in ballistic impact. Therefore, it can cause higher energy dissipation when the impact velocity increases substantially even the impact energy unchanged.

3.4. Energy dissipation mechanism

The energy dissipation of the sandwich structure is contributed by the damage of Kevlar face sheets and the SP core. Due to the impact of the projectile or the impactor, the huge deformation in Kevlar and the partial fracture of the fabric yarns contribute the energy dissipation (Fig. 6 and Movie S1-S3). During the process, the transverse stress is diffused and attenuated through the friction of the fabric yarns. The friction between the yarns in a Kevlar fabric is so weak that the transverse stress mainly propagates along the stretched yarns directly (Fig. 10(a)). So there are obviously stretched traces in the horizontal and vertical directions of the penetrated holes after impact (Fig. 10(d)). For Kevlar/SP/Kevlar, SP adheres to the fabric and immerses in the gaps. The friction between the yarns is strengthened, which is beneficial to the transverse stress propagates to the surroundings, reduce stress concentration and dissipate more impact energy (Fig. 10(b)). So the stretched traces cannot be observed in Fig. 10(e). The energy dissipation contributed by the SP core is because of the significant shear-hardening behavior of SP caused by the "B-O cross bonds". Moreover, with increasing of the $CaCO_3$ content, the friction between the projectile and $CaCO_3$ particles, and among the Kevlar fabrics increases, thus the energy dissipation effect increased, especially in the ballistic impact. Therefore, the energy dissipation is much higher when the sandwich structure suffers ballistic impact or the content of $CaCO_3$ is higher (Fig. 9).

Fig. 10(f) shows the schematic of the microscopic structure of SP (white points represent $CaCO_3$ particles) and Fig. 10(g) shows the "B-O cross bonds" (black points) formed from the react of boric acid and dimethylsiloxane at high temperature. As mentioned by Seetapan N [18] and Wang S [30], the O atoms in the Si-O structure could share their valence shell electrons with the p-orbital of B atoms and the formed "B-O cross bonds" between long molecular chains are transient, dynamically variable and vulnerable similar to hydrogen bonds. If SP is excited by an external force with low rates, the molecular chains have enough time to disentanglement and display the soft behavior. However, if the external stress is at a high rate like a drastic impact, the "B-O cross bonds" cannot be broken and the long molecular chains are entangled with each other to form a locked crosslinked polymer network. In this case, when the longitudinal stress spread to SP in the impact testing, SP turns into solid-liked state immediately. The stress is dispersed and attenuated during the impact (Fig. 10(c)). Therefore, a great amount of SP is broken into powder leading to lots of energy dissipated.

Additionally, the filled $CaCO_3$ particles (Fig. 10(g)) and the SP polymer matrix form additional physical crosslinking owing to the evolution of molecular interactions [32]. So with increasing of the content $CaCO_3$ in SP, the storage modulus and impact resistance increase. Moreover, when the projectile or impactor pass through the SP layer, the friction between the projectile or impactor and $CaCO_3$ particles causes a part of energy dissipation. The fiction will be larger and cause more energy dissipation if the content of $CaCO_3$ is higher or the impact velocity is faster. Therefore, under ballistic impact, the SP core contributed more influence on the energy dissipation than in the low velocity impact.

4. Conclusions

In this work, a soft sandwich structure with two layer Kevlar face sheets and one SP core was fabricated. $CaCO_3$ particles were

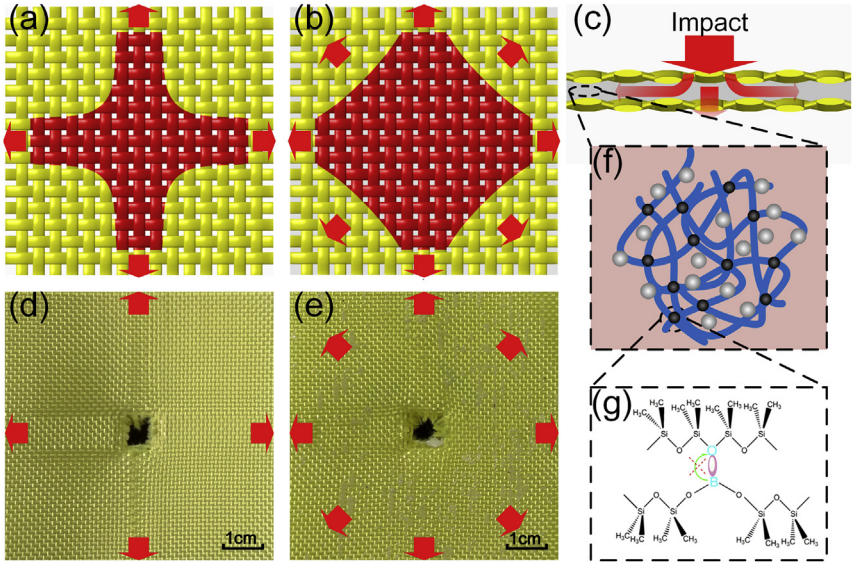

Fig. 10. Schematic of the propagation of the transverse stress in the fabric layer: (a) neat fabric and (b) fabric adhered with SP, and (c) the propagation of the longitudinal stress in SP; the photographs of the front face of (d) Kevlar/Kevlar and (e) Kevlar/SP-$CaCO_3$-20%/Kevlar; (f) the microscopic structure of SP with $CaCO_3$ particles and (g) the "B-O cross bonds".

used to improve the strength and modulus of SP. The storage modulus of SP increased by 2–3 orders of magnitude (up to 1.86 MPa) with increasing of the shear frequency indicating the shear-hardening property. The results of ballistic impact tests indicated Kevlar/SP/Kevlar could resist ballistic impact at a higher velocity and dissipate more energy than Kevlar/Kevlar. There was about 60% increment of the energy dissipation when the core was SP with the highest content of $CaCO_3$. By using the high-speed video camera, it was observed that a lot of SP was cracked and ejected like powders which dissipated a large of impact energy. For Kevlar/SP-$CaCO_3$-50%/Kevlar, the energy dissipation under ballistic impact increased 63% than under the low velocity impact with the same impact energy due to the shear-hardening effect. In addition, the similarities between the rheological test and impact test results indicated that the storage modulus of SP could be used as a tool to estimate the energy dissipation capacity of the sandwich structure with SP core. At last, the "B-O cross bonds" and crosslinked polymer network are believed to be the reason for the reliable stress dispersion and attenuation. The excellent protection performance illustrates it can be well applied in personal body armors and further work will be done to investigate the detailed mechanism.

Acknowledgments

Financial support from the National Natural Science Foundation of China [Grant No. 11372301, 11772320]; the Fundamental Research Funds for the Central Universities [WK2480000002]; and the Strategic Priority Research Program of the Chinese Academy of Sciences [Grant No. XDB22040502] is gratefully acknowledged. This study was also supported by the Collaborative Innovation Center of Suzhou Nano Science and Technology.

Appendix A. Supplementary data

Supplementary data related to this article can be found at https://doi.org/10.1016/j.compscitech.2017.10.019.

References

[1] H.N.K.T. Palleti, S. Gurusamy, S. Kumar, R. Soni, B. John, R. Vaidya, A. Bhoge, N.K. Naik, Ballistic impact performance of metallic targets, Mater Des. 39 (2012) 253–263.
[2] Z.H. Tan, X. Han, W. Zhang, S.H. Luo, An investigation on failure mechanisms of ceramic/metal armour subjected to the impact of tungsten projectile, Int. J. Impact Eng. 37 (12) (2010) 1162–1169.
[3] S. Atiq, R.D. Rawlings, A.R. Boccaccini, Behaviour of a commercial wired glass under low energy ballistic impact, Glass Sci. Technol. 77 (1) (2004) 31–35.
[4] M. Hudspeth, A. Agarwal, B. Andrews, B. Claus, F. Hai, C. Funnell, J. Zheng, W.N. Chen, Degradation of yarns recovered from soft-armor targets subjected to multiple ballistic impacts, Compos A-Appl Sci. Manuf. 58 (2014) 98–106.
[5] H.S. Hwang, M.H. Malakooti, B.A. Patterson, H.A. Sodano, Increased interyarn friction through ZnO nanowire arrays grown on aramid fabric, Compos Sci. Technol. 107 (2015) 75–81.
[6] P.F. Wang, J.L. Yang, W.S. Liu, X.Z. Tang, K. Zhao, X.H. Lu, S.L. Xu, Tunable crack propagation behavior in carbon fiber reinforced plastic laminates with polydopamine and graphene oxide treated fibers, Mater Des. 113 (2017) 68–75.
[7] A. Manero, J. Gibson, G. Freihofer, J.H. Gou, S. Raghavan, Evaluating the effect of nano-particle additives in Kevlar® 29 impact resistant composites, Compos Sci. Technol. 116 (2015) 41–49.
[8] A.K. Bandaru, V.V. Chavan, S. Ahmad, R. Alagirusamy, N. Bhatnagar, Ballistic impact response of Kevlar® reinforced thermoplastic composite armors, Int. J. Impact Eng. 89 (2016) 1–13.
[9] E.E. Haro, J.A. Szpunar, A.G. Odeshi, Ballistic impact response of laminated hybrid materials made of 5086-H32 aluminum alloy, epoxy and Kevlar® fabrics impregnated with shear thickening fluid, Compos A-Appl Sci. Manuf. 87 (2016) 54–65.
[10] Z.H. Tan, L. Zuo, W.H. Li, L.S. Liu, P.C. Zhai, Dynamic response of symmetrical and asymmetrical sandwich plates with shear thickening fluid core subjected to penetration loading, Mater Des. 94 (2016) 105–110.
[11] O.E. Petel, S. Ouellet, J. Loiseau, D.L. Frost, A.J. Higgins, A comparison of the ballistic performance of shear thickening fluids based on particle strength and volume fraction, Int. J. Impact Eng. 85 (2015) 83–96.
[12] C.D. Cwalina, C.M. McCutcheon, R.D. Dombrowski, N.J. Wagner, Engineering enhanced cut and puncture resistance into the thermal micrometeoroid garment (TMG) using shear thickening fluid (STF) - armor (TM) absorber layers, Compos Sci. Technol. 131 (2016) 61–66.
[13] Y.S. Lee, E.D. Wetzel, N.J. Wagner, The ballistic impact characteristics of Kevlar® woven fabrics impregnated with a colloidal shear thickening fluid, J. Mater Sci. 38 (13) (2003) 2825–2833.
[14] B.W. Lee, I.J. Kim, C.G. Kim, The influence of the particle size of silica on the ballistic performance of fabrics impregnated with silica colloidal suspension, J. Compos Mater 43 (23) (2009) 2679–2698.
[15] D.P. Kalman, R.L. Merrill, N.J. Wagner, E.D. Wetzel, Effect of particle hardness on the penetration behavior of fabrics intercalated with dry particles and concentrated particle-fluid suspensions, ACS Appl. Mater Interfaces 1 (11) (2009) 2602–2612.
[16] Y. Park, Y. Kim, A.H. Baluch, C.G. Kim, Numerical simulation and empirical comparison of the high velocity impact of STF impregnated Kevlar fabric using friction effects, Compos Struct. 125 (2015) 520–529.
[17] C.S. Boland, U. Khan, G. Ryan, S. Barwich, R. Charifou, A. Harvey, C. Backes, Z. Li, M.S. Ferreira, M.E. Mobius, R.J. Young, J.N. Coleman, Sensitive electromechanical sensors using viscoelastic graphene-polymer nanocomposites, Science 354 (6317) (2016) 1257–1260.
[18] N. Seetapan, A. Fuongfuchat, D. Sirikittikul, N. Limparyoon, Unimodal and bimodal networks of physically crosslinked polyborodimethylsiloxane: viscoelastic and equibiaxial extension behaviors, J. Polym. Res. 20 (7) (2013) 183.
[19] T.F. Tian, W.H. Li, J. Ding, G. Alici, H. Du, Study of shear-stiffened elastomers, Smart Mater Struct. 21 (12) (2012).
[20] R. Martin, A. Rekondo, A.R. de Luzuriaga, A. Santamaria, I. Odriozola, Mixing the immiscible: blends of dynamic polymer networks, RSC Adv. 5 (23) (2015) 17514–17518.
[21] J. Liang, X.H. Zhang, Rheological properties of SP in shock transmission application, J. Mater Civ. Eng. 27 (9) (2015) 04014250.
[22] W.F. Jiang, X.L. Gong, S. Wang, Q. Chen, H. Zhou, W.Q. Jiang, S.H. Xuan, Strain rate-induced phase transitions in an impact-hardening polymer composite, Appl. Phys. Lett. 104 (12) (2014) 121915.
[23] S. Wang, S.H. Xuan, Y.P. Wang, C.H. Xu, Y. Mao, M. Liu, L.F. Bai, W.Q. Jiang, X.L. Gong, Stretchable polyurethane sponge scaffold strengthened shear stiffening polymer and its enhanced safeguarding performance, ACS Appl. Mater Interfaces 8 (7) (2016) 4946–4954.
[24] Z.H. Tan, H.H. Luo, W.G. Long, X. Han, Dynamic response of clamped sandwich beam with aluminium alloy foam core subjected to impact loading, Compos B-Eng 46 (2013) 39–45.
[25] A.Q. Dayo, B.C. Gao, J. Wang, W.B. Liu, M. Derradji, A.H. Shah, A.A. Babar, Natural hemp fiber reinforced polybenzoxazine composites: curing behavior, mechanical and thermal properties, Compos Sci. Technol. 144 (2017) 114–124.
[26] M.R. O'Masta, B.G. Compton, E.A. Gamble, F.W. Zok, V.S. Deshpande, H.N.G. Wadley, Ballistic impact response of an UHMWPE fiber reinforced laminate encasing of an aluminum-alumina hybrid panel, Int. J. Impact Eng. 86 (2015) 131–144.
[27] N. Jover, B. Shafiq, U. Vaidya, Ballistic impact analysis of balsa core sandwich composites, Compos B-Eng 67 (2014) 160–169.
[28] Standard NIJ 0101.04, Ballistic Resistance of Personal Body Armor, 2000. Washington DC, USA.
[29] Specification Detail, Projectile, Calibers .22, .30, .50, and 20 Mm Fragment-simulating, MIL-dtl-46593B (MR), 2006.
[30] S. Wang, W.Q. Jiang, W.F. Jiang, F. Ye, Y. Mao, S.H. Xuan, X.L. Gong, Multifunctional polymer composite with excellent shear stiffening performance and magnetorheological effect, J. Mater Chem. C 2 (34) (2014) 7133–7140.
[31] B. Song, H. Park, W.Y. Lu, W.N. Chen, Transverse impact response of a linear elastic ballistic fiber yarn, J. Appl. Mech. 78 (5) (2011) 051023.
[32] X.M. Xu, Y.H. Song, Q. Zheng, G.H. Hu, Influence of incorporating $CaCO_3$ into room temperature vulcanized silicone sealant on its mechanical and dynamic rheological properties, J. Appl. Polym. Sci. 103 (3) (2007) 2027–2035.